

A genetic-based effective approach to path-planning of autonomous underwater glider with upstream-current avoidance in variable oceans

Chien-Chou Shih^{1,2} · Mong-Fong Horng¹ · Tien-Szu Pan¹ · Jeng-Shyang Pan³ · Chun-Yu Chen¹

Published online: 5 April 2016
© Springer-Verlag Berlin Heidelberg 2016

Abstract In this work, an exponential effective function (EEF) is developed as fitness function applied in a hybrid-Genetic Algorithm (hybrid-GA) to propose a genetic-based effective approach to the glider path-planning of ocean-sampling mission in variable oceans. The proposed EEF is such an objective function that is able to be implemented in optimization algorithm such as Genetic Algorithm (GA) for evaluation of the fittest path. In consideration of the glider path-planning problem (GPP), two motivations are driven by the proposed approach to the glider path-planning in discovery of: (1) a reachable path with the upstream-current avoidance (UCA) in variable oceans; (2) an efficient path for the glider ocean-sampling mission. The exponential combination of the glider motion and current effects as well as the cruising distance benefits the path in terms of reachability and efficiency. The reachability is the first motivation

to discover a reachable path implemented by the scheme of UCA, while the efficiency is the second motivation to shorten the cruising distance. Meanwhile, the stabilized path solution is accomplished by hybrid-GA. In variable oceans, currents severely impact the path solution and lead the global optimum to absence. Therefore, alternative is to discover an optimal path with the minimum upstream-current sub-paths to approximate the minimal cruising distance in the condition that the discovered cruising distance should be less than the glider cruising range. To deeply analyze the path reachability, two theorems are developed to verify the conditions of the downstream-current angle (DCA). To evaluate the path-planning performances, 6 state-of-the-art fitness functions are studied and used to make a fair comparison with the EEF in hybrid-GA. First of all, 112 scenarios are created in the restricted random current variations (RRCV). Secondly, 21 scenarios are created in the near-real Kuroshio Current of east Taiwan (KCET) introducing from an ocean prediction model. These scenarios are designed to evaluate fairly the EEF in hybrid-GA. Numeric results show that whether the RRCV or the KCET, the proposed EEF indeed is able to discover the optimal path with the benefits of reachability and efficiency. Therefore, the proposed genetic-based effective approach is well developed to solve the GPP in variable oceans.

Communicated by V. Loia.

✉ Mong-Fong Horng
mfhorng@cc.kuas.edu.tw

Chien-Chou Shih
raymondshih@narlabs.org.tw

Tien-Szu Pan
tpan@cc.kuas.edu.tw

Jeng-Shyang Pan
jengshyangpan@fjut.edu.cn

Chun-Yu Chen
ccyfish@gmail.com

¹ Department of Electronic Engineering, National Kaohsiung University of Applied Sciences, Kaohsiung, Taiwan

² Taiwan Ocean Research Institute, National Applied Research Laboratories, Kaohsiung, Taiwan

³ School of Information Science and Engineering, Fujian University of Technology, Fujian Province, China

Keywords Optimization · Genetic Algorithm · Autonomous underwater glider · Path-planning · Exponential effective function · Upstream-current avoidance

1 Introduction

Autonomous underwater glider (AUG) is a buoyancy-driven underwater vehicle, which is a type of autonomous underwater vehicle (AUV). The wings convert the lift and drag forces

to produce the forward moving with a half of a knot speed passing through the water columns. The rudder is used to turn the glider heading. By rolling and shifting the internal masses or batteries, the gravity and attitude can be controlled. The buoyancy-driven engine benefits the low-power consumption. However, without active propeller, the glider is difficult to overcome the variable currents. An efficient and reachable path-planning approach, therefore, is essential to benefit the glider ocean-sampling mission and to greatly reduce the tedious path-planning by hand in variable oceans.

In the last decade, the topics related to find an optimal path for AUV have been studied. [Young and Wan \(2013\)](#) conducted rapidly-exploring random trees (RRT)-based local path-planning for AUV. RRT is one of the path-planning algorithms that attempt to rapidly and uniformly explore the solution space, offering benefits that are similar to those obtained by other successful randomized planning methods ([LaValle and Kuffner 2000](#)). However, the environments with low connectivity due to the presence of obstacles can severely affect convergence ([Clifton et al. 2008](#)). The low-connective environments such as ship lanes, strong and dynamic currents critically increase the path-planning complexity and lead the path to unreachability. [Fernandez-Perdomo et al. \(2010\)](#) developed new path-planning software named Pinzon to assist underwater vehicles piloting. The proposed software integrated a novel path-planning algorithm called constant-time surfacing A* (CTS-A*) that is particularly useful for the long-range glider missions. A* algorithm is Dijkstra-like search heuristic, which prescribes how to use such information from a problem domain to guarantee a minimum cost path solution through a graph ([Hart et al. 1968](#)). In fact, A* is a guided version of breadth-first search, which is exponential in memory complexity with respect to the length of the solution. Classic algorithms such as RRT and Dijkstra-like algorithms only concern with the constant environment; however, the upstream-current (UC) conditions had not been considered in their search heuristic.

In this work, a novel problem of the GPP is studied. In the GPP, there is a challenge to design an objective function to benefit a path in terms of reachability and efficiency. In other words, the characteristics such as the glider motion and the cruising distance, as well as the variable currents, should be considered in the objective function and integrated into an optimization algorithm to build a path-planning approach. Therefore, the EEF is developed as a new fitness function based on these characteristics applied in hybrid-GA that is able to discover a reachable and efficient path and to stabilize the path solution in the GPP. The exponential combination of the EEF is a premium method which emphasizes obviously the benefits of reachability and efficiency. Besides, GA is one of the well-known optimization algorithms, which is easy to involve arbitrary objective functions in it. Thus, in this work, the EEF applied in hybrid-GA is able to develop a premium

path-planning approach for the glider ocean-sampling mission in variable oceans.

The rest of this paper is organized as follows. Related works on literature reviews of optimization algorithm and problem statement of the glider path-planning are studied in Sect. 2. Development of genetic-based effective path-planning approach with the EEF and new theorems in conditions of the downstream-current (DC), as well as study on the optimal path of the GPP are described in Sect. 3. In Sect. 4, two current variations are created to simulate the total 133 scenarios and all scenarios are made fair comparisons with fair GA configurations. Finally, conclusions are discussed in Sect. 5.

2 Related works

2.1 Literature review on optimization algorithms

In computer science, heuristic methods such as RRT and A* are well-known algorithms which are able to solve the optimization problems such as path-planning and task scheduling. However, RRT and A* lack for path-planning in changing environment ([Alcázar et al. 2011](#); [Bhadoria and Singh 2014](#); [Zhang and Zhao 2014](#)). In the field of evolutionary computation, GA is an optimization technique which is routinely used to generate useful solutions to optimization problems. In [Ahmed and Deb \(2013\)](#), [Castillo et al. \(2007\)](#), [Hong et al. \(2002\)](#), [Alvarez et al. \(2004\)](#), [Moura et al. \(2010\)](#), [Aghababa \(2012\)](#), GA has been studied in underwater vehicle path planning with high flexibility and applicability and validated as an efficient optimization algorithm with less memory and real-time demand to solve the optimization problem. Therefore, GA is accepted as the optimization algorithm to involve the EEF for solving the GPP in this work. GA mimics the process of natural selection inspired by natural evolutions including reproduction, crossover and mutation, as well as searching the space of chromosomes in a way much more subtle than a “random search with preservation of the best ([Holland 1984](#)). GA provides a flexible and efficacious path-planning approach with arbitrary objective functions to discover the optimal paths. A simple GA process includes population initialization, fitness evaluation, selection and reproduction. The search space of GA is represented as a collection of individuals which are encoded as fixed length bit strings referred to as chromosomes ([Laraña et al. 1999](#)). GA employs a population of individuals as the possible solutions of a problem. Meanwhile, a good individual has more chances to be selected into the mating pool so that it has more chances to mate than low-quality individuals have ([Yu and Gen 2010](#)). GA randomly generates a set of individuals and each individual comes with a particular fitness evaluated by the fitness function. The population size

and individual length are dependent on the problem complexity. A complete iteration so-called a generation consists of all GA processes. A run is defined as when a given amount of iterations is completed.

In evolution strategy of GA, a fitness function is significant to evaluate the fittest path. A fitness function is a particular type of objective function, which is used to evaluate the fittest in a problem. Classic objective functions such as K -means, C -means, Euclidean distance and kinematic motion model are capable of the fitness functions for GA. The fitness resulted by fitness function illustrates that how good a solution can be promoted to an outstanding one. In this work, 6 state-of-the-art objective functions are studied. Alvarez et al. (2004) developed a kinematic model-based energy cost (EC) function to compute the strength of the individuals that the energy cost required to run each path. Fernandez-Perdomo et al. (2011) computed an underestimated temporal cost to reach the goal from the current location using the straight-line distance to the goal and proposed a conservative but admissible heuristic function to compute a reaching cost (RC). Pêtrès et al. (2007) proposed a heuristic function that estimates the residual distance between the considered current location and the goal location with a constant α . When constant α equals to 1, heuristic function of hybrid search (HS) is likely an A* algorithm. Shih et al. (2014) considered the glider motion with the current effects and total cruising distance to develop an effective function (EF) and applied the EF in GA. Shih et al. (2012) proposed an effective speed (ES) function to compute the composite speed of the glider velocity and current velocity, as well as the drift factor for the glider path-planning. Soullignac (2011) combined an appropriate objective function of actual travel time (ATT) in a Dijkstra-like algorithm that guarantees the existence of a path with an arbitrary precision. These functions mentioned above are well-designed objective functions to support the path-planning approaches to the specific path-planning problem. However, some parameters such as the distance and effective angle between the glider heading and the current direction were not considered as well. For instance, EF, ES and ATT did not consider the adjacent distance; while RC and HS did not concern with the effective angle. Even though these functions concerned the variable currents; however, they missed the consideration of the UC on the way to target. In fact, the UC greatly affects the path reachability.

Considering buoyancy-driven engine features, the power-saving glider moves like a saw-tooth profile with a half of knot velocity so that it can prolong the cruising range from least weeks to months. However, currents are classified as variable and unknown environment that essentially influences the path-planning performance of a slow-moving glider. Moreover, currents lead the glider mission to failure, even endanger the glider. Consider that the slow-moving glider is difficult to confront stronger currents than its

velocity, a premium path-planning approach to the glider ocean-sampling mission should concern completely the current effects to discover a reachable and efficient path as possible as it can. Thus, the objective of this work is to develop a fitness function of the EEF applied in hybrid-GA as a premium path-planning approach to solve the GPP in variable oceans. The EEF combines the glider motion and current effects as well as the cruising distance carefully so that it can benefit the optimal path with reachability and efficiency in the ocean-sampling mission.

2.2 Problem statement on AUG path-planning

The ocean-sampling is an activity to observe and collect oceanographic properties in an ocean area where there are interests in the ocean research for scientists. These interests are such as climate change associated with Kuroshio Current that scientists create an ocean-sampling mission and deploy scientific instruments to collect data in that area. In the glider ocean sampling, a mission means that given a set of waypoints in the ocean area of interest, a glider with the limited cruising range cruises autonomously in the programmed water depth and reaches to each waypoint once and only once from the source to the target. The glider follows a prior path-planning with a series of waypoints and reaches the next waypoint one by one to carry out the desired goal of a mission. A path is connected by a series of waypoints in an ocean area. In case of n waypoints, there will be $(n-1)!$ candidate solutions to be solved in the GPP. Thus, the GPP is also a NP-hard (non-deterministic polynomial-time hard) problem. Most path-planning approaches assume that the environment is constant; however, it is not applicable in real oceans. Typically, the discovery of a path with the constant environment can be considered as a simple traveling salesman problem (sTSP). However, to find a path with the variable currents can be considered as a complicated TSP (cTSP). The GPP, therefore, is a cTSP-like optimization problem.

In graph theory, reachability refers to the ability to travel from a vertex to a specific vertex within a directed graph $G = (S, E)$. S is a set of vertices, while E is a set of edges. A vertex s can reach a vertex t if there exists a sequence of adjacent vertices (Skiena 2008) which starts with s and ends with t . In this work, a waypoint can be considered as a vertex. Self-looping should not be allowed in this work. Thus, the glider starts at the source waypoint ($wp_{s=0, s \in S}$), passes through intermediate waypoint ($wp_{q \in S}$) once and only once, and finally terminates at the target waypoint ($wp_{t \in S}$) which is determined by scientist or the path-planning approach. The great-circle (GC) formula (NIMA 2002) is used to calculate the distance between two waypoints on the earth surface, given by

$$d_{GC} = WGS84_a \times \cos^{-1} [\cos \phi_1 \cos \phi_2 \cos(\lambda_1 - \lambda_2) + \sin \phi_1 \sin \phi_2] \quad (1)$$

where d_{GC} is the distance between two arbitrary waypoints in a gnomonic projection; $WGS84_a$ is the equatorial radius about 6378 km; λ and ϕ are the longitude and latitude, respectively. A waypoint with coordinates is denoted by $wp(\lambda, \phi)$.

In optimization problem, the GPP is a problem between TSP and navigation problem. Original TSP is denoted by messenger problem which is a task to find the shortest route connecting the points for finitely many points whose pairwise distances are known (Schrijver 2005). In other words, the problem of TSP is “given a set of cities (points) and a known pairwise distance matrix, finding the shortest path that the salesman travels each city exactly once and then returns to the original city”. The other optimization problem related to the GPP is the problem of motion planning, also known as the navigation problem, which frequently refers to motions of a robot in a 2D or 3D world that contains obstacles. A motion planning involves determining what motions are appropriate for the robot so that the robot reaches a goal state without colliding into obstacles (LaValle 2006). The navigation problem is to produce a continuous motion that connects source s and target t , while avoiding collision with known obstacles. The kinodynamic planning problem is a class of navigation problems, which is to synthesize a robot motion subject to simultaneous kinematic constraints such as avoiding obstacles, and dynamic constraints such as modulus bounds on velocity, acceleration and force (Donald et al. 1993). Unlike TSP, the glider does not return to the source waypoint. Moreover, these constraints of navigation problem such as obstacles and acceleration are not concerned with this work. Besides, TSP and navigation problem do not consider the environmental variation in the path-planning problem. Assume that the glider does not cruise in ship lane and no physical obstacle exists on the way to target. Thus, the glider path-planning in the variable currents is considered as a novel problem called the GPP, which is a problem of how to discover an optimal path from a source waypoint wp_s to a target waypoint wp_t through each intermediate waypoint wp_q once and only once.

To represent an individual for the GPP, a permutation encoding is applicable to ordering problems and used to describe a path sequence in an individual of GA. Given a set of waypoints S , each waypoint $wp_{i \in S}$ is indexed a unique integer i . The source waypoint is denoted by wp_0 , while the target waypoint is decided by the optimization algorithm or scientists. Thus, an individual is represented by

$$\mathbf{I}_k \in \mathbf{P} = \{wp_{i \in S}, \text{ for } 0 \leq i \leq n - 1\} \quad (2)$$

where \mathbf{I}_k is the k th individual in the population set \mathbf{P} ; wp_i is the i th waypoint and n is the number of waypoints. In

case of the path with 8 waypoints in a mission, a permutation encoding of an individual could be represented as $\{0, 7, 4, 6, 3, 5, 1, 2\}$. Subsequently the goals of this work are to: (1) develop a new EEF as a fitness function to combine the glider motion with the current effects; (2) implement the EEF for hybrid-GA to discover an optimal path with the UCA in the variable currents; (3) develop new theorems to derive the conditions of the UCA.

3 A genetic-based effective approach to AUG path-planning with upstream-current avoidance in variable oceans

3.1 Design of genetic-based path-planning approach

GA is an iterative- and evolutionary-based optimization algorithm to find the individual from the search space with the best genetic material. The search space of a problem is represented as a collection of individuals. Classic GA uses crossover and mutation operators with stochastic rates to create the solution diversity and escape the local optima. In this work, multiple crossover and mutation operators are applied in hybrid-based GA. Crossover operators include partially mapped crossover (PMX) and partially scrambling crossover (PSX), while mutation operators include exchange mutation (EM), rotate mutation (RM) and inversion mutation (IVM). In general, GA configuration including crossover and mutation rates, iteration and population sizes as well as run size should be declared in GA initialization process.

In fact, determination of the appropriate crossover and mutation rates is not only a critical but also an open issue because the results are highly depending on the optimal goal of a problem. There is no general rule in assignment of crossover and mutation rates for the most problems. Typical mutation rate with a low value between 0 and 1 % works well when the population size is large enough. However, for the efficient computation with less memory and real-time demand, a small population size and high mutation rate are preferred. Moreover, when a portion of individuals is trapped in local optimum, high mutation rate is a useful strategy to increase the population diversity and to enhance the ability of exploring other possible solution. To determine crossover and mutation rates, a trial is exercised iteratively. Both crossover and mutation rates are given from 0 to 100 % stepped by 10 %. In this trial, the path solution is converged when crossover and mutation rates are equivalent to 10 and 20 %, respectively. Thus, the accepted crossover and mutation rates of this work are 10 and 20 %, respectively. Besides, high mutation rate is also a useful strategy to reduce the population size in this work.

Table 1 A survey for GA configurations

WPs	Popu.	Iter.	Run	Mission type	Path cost	UCA	Crossover	Mutation	Test cases
52–442 (Albayrak and Allahverdi 2011)	40	20,000	N/A	sTSP	Distance	Non	DPX	GSTM	336
10 (Majumdar and Bhunia 2011)	20	50	20	sTSP	Time	Non	MOX MCX SX	EM RM	12
15 (Majumdar and Bhunia 2011)	30	50	20	sTSP	Time	Non	MOX MCX SX	EM RM	12
20 (Majumdar and Bhunia 2011)	40	50	20	sTSP	Time	Non	MOX MCX SX	EM RM	12
30 (Majumdar and Bhunia 2011)	60	50	20	sTSP	Time	Non	MOX MCX SX	EM RM	12
17–443 (Nagata and Soler 2012)	100–300	N/A	100	sTSP	Distance	Non	EAX	N/A	153
> 100 (Wang 2014)	20	100	N/A	sTSP	Distance	Non	PBX	EM	30
101–200 (Wang 2014)	100	200	N/A	sTSP	Distance	Non	PBX	EM	45
201–300 (Wang 2014)	100	200	N/A	sTSP	Distance	Non	PBX	EM	18
301–500 (Wang 2014)	50	200	N/A	sTSP	Current	Non	PBX	EM	15
6–12 (Groba et al. 2015)	100	1000	N/A	cTSP	Time, current	Non	GX	EM	17
29–198 (Ahmed 2010)	200	1000	10	sTSP	Distance	Non	SCX	EM	45

DPX distance preserving crossover, MOX modified order crossover, MCX modified cycle crossover, SX sequence crossover, EAX edge assembly crossover, PBX position-based crossover, GX greedy crossover, SCX sequential constructive crossover, GSTM greedy sub tour mutation, EM exchange mutation; RM replacement mutation

Table 2 GA configurations

Waypoints	5	9	10	16	32	35	48
Crossover rate (%)	10	10	10	10	10	10	10
Mutation rate (%)	20	20	20	20	20	20	20
Population	20	50	50	100	200	200	300
Iteration	50	100	100	200	300	400	500
Run	20	20	20	20	30	40	40

The remaining GA configuration of population and iteration sizes as well as run size is highly dependent on the problem complexity such as the number of waypoints. To determine the remaining GA configuration, literatures (Albayrak and Allahverdi 2011; Majumdar and Bhunia 2011; Nagata and Soler 2012; Wang 2014; Groba et al. 2015; Ahmed 2010) are surveyed and summarized in Table 1. These cited papers assigned various population and iteration sizes as well run size to solve different path-planning problem and to reach the desired goals in various environments. Besides, these cited papers used adequate population sizes to solve their problems. Thus, conclusion of this survey; the GA configurations accepted for simulations with various waypoints in this work are given in Table 2.

3.2 Development of exponential effective function with upstream-current avoidance

Typically, the kinematic motion model is basic method which is used to formulate the composite velocity between the vehi-

cle motion and the current effects. Mathematically, the forward kinematic equations define a function between the space of Cartesian positions and orientations and the space of joint positions (Spong and Vidyasagar 2008). In this paper, the unconstrained kinematic motion model (Fernandez-Perdomo et al. 2011) is used to describe the relative velocity relations between the glider and currents, given by

$$\vec{v}_e \triangleq \vec{v}_g + \vec{v}_c \tag{3}$$

where \vec{v}_e , \vec{v}_g and \vec{v}_c are the vectors of the glider, current and effective velocities, respectively. Navigation problem is described as “let a vessel traveling at constant speed on a body of water having surface velocity (Weisstein 2002)” that can be simply modeled by a kinematic motion model. Kinematic motion model only describes the composite velocity relations between the glider motion and current effects; however, the angle between the glider heading and the current direction is not considered properly. Assume that the current effects are always present in a path; that means, the current velocity is a

non-zero value. To consider the glider motion with the current effects completely, a cruising capability (CC) is developed as the first component of the EEF to benefit the path reachability, given by

$$\varepsilon_j = \frac{|\vec{v}_g|}{|\vec{v}_{c_j}|} \times \cos(\theta_{ec_j}), \theta_{ec_j} = \theta_{g_j} - \theta_{c_j} \tag{4}$$

where ε_j is the CC; \vec{v}_g and \vec{v}_{c_j} are the velocity vectors of the glider and currents, respectively; θ_{ec_j} is the effective angle between the glider heading θ_{g_j} and the current direction θ_{c_j} ; j is the j th sub-path. The glider heading is toward to the next waypoint from its current waypoint. The CC has the maximal performance when the glider cruises actually along with the DC. To consider the distance efficiency, an adjacent degree (AD) is developed as the second component of the EEF to benefit the path efficiency, given by

$$\xi_j = \frac{d_{GC_j}}{d_{total}} \tag{5}$$

where ξ_j and d_{GC_j} are the AD and the distance on the j th sub-path, respectively. d_{total} is the cruising distance in a path, given by

$$d_{total} = \sum_{j=0}^{n-2} d_{GC_j} \tag{6}$$

Equation (5) shows that the higher the AD is, the longer distance on the j th sub-path we have. Afterward, an exponential combination is a premium method to integrate the benefits of CC and AD in a sub-path, given by

$$eef_j = \varepsilon_j \times \exp(-\alpha \times \varepsilon_j \times \xi_j), \text{ for } 0 \leq \alpha \leq 1 \tag{7}$$

where eef_j is the fitness of the EEF on the j th sub-path; α is the curve shaping (CS) parameter which enables the scheme of UCA and benefits the path reachability. The detailed CS parameter is investigated in Sect. 3.3. Finally, the fitness of

a path is given by

$$eef = \sum_{j=0}^{n-2} eef_j \tag{8}$$

where eef is the fitness of the EEF in a path. The EEF is developed as a fitness function to evaluate the path reachability and efficiency in hybrid-GA to discover the optimal path for solving the GPP.

3.3 Activation of upstream-current avoidance

The CS parameter with the positive value between 0 and 1 is designed to raise the reachability in a path. When CS parameter is equal to zero, the scheme of UCA is disabled and only CC is involved in the EEF to evaluate the path. Otherwise, the CS is used to enable the scheme of UCA and to shape the effective curve of the EEF, as shown in Fig. 1. The effective curve related to the effective angle and the AD is showed in Fig. 1a. There are two conditions that cause eef to be dropped deeply. The first condition is held when the sub-path has high AD; that means, this sub-path has a long distance. The second condition is held when the glider heading and the current direction are in the opposite direction; that means, the glider confronts the UC. In case of a sub-path with high AD and along with the UC ($\theta_{ec} = 180^\circ$), as shown by the blue line, the solved eef resulted in extreme negative value and this sub-path will be considered as an unreachable one. However, in case of a sub-path with high AD and along with the DC ($\theta_{ec} = 0^\circ$), as shown by the green line, the solved eef is always higher than the blue line one so that this sub-path along with the DC is always considered as the reachable one. These two cases mentioned above are given the same CS parameter ($\alpha = 1.0$).

For the glider safety, the sub-path with high AD and along with the DC should be considered as the better sub-path than the sub-path with small AD but along with the UC. However, the sub-path may be considered as an unreachable one when this sub-path is with high AD and along with the DC ($\theta_{ec} = 0^\circ$) but given a median CS parameter ($\alpha = 0.5$), as shown

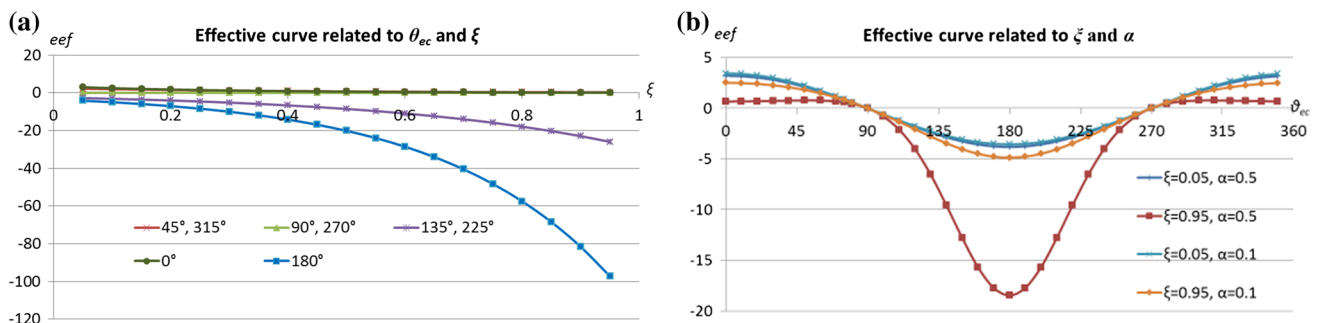


Fig. 1 Effective curve for EEF

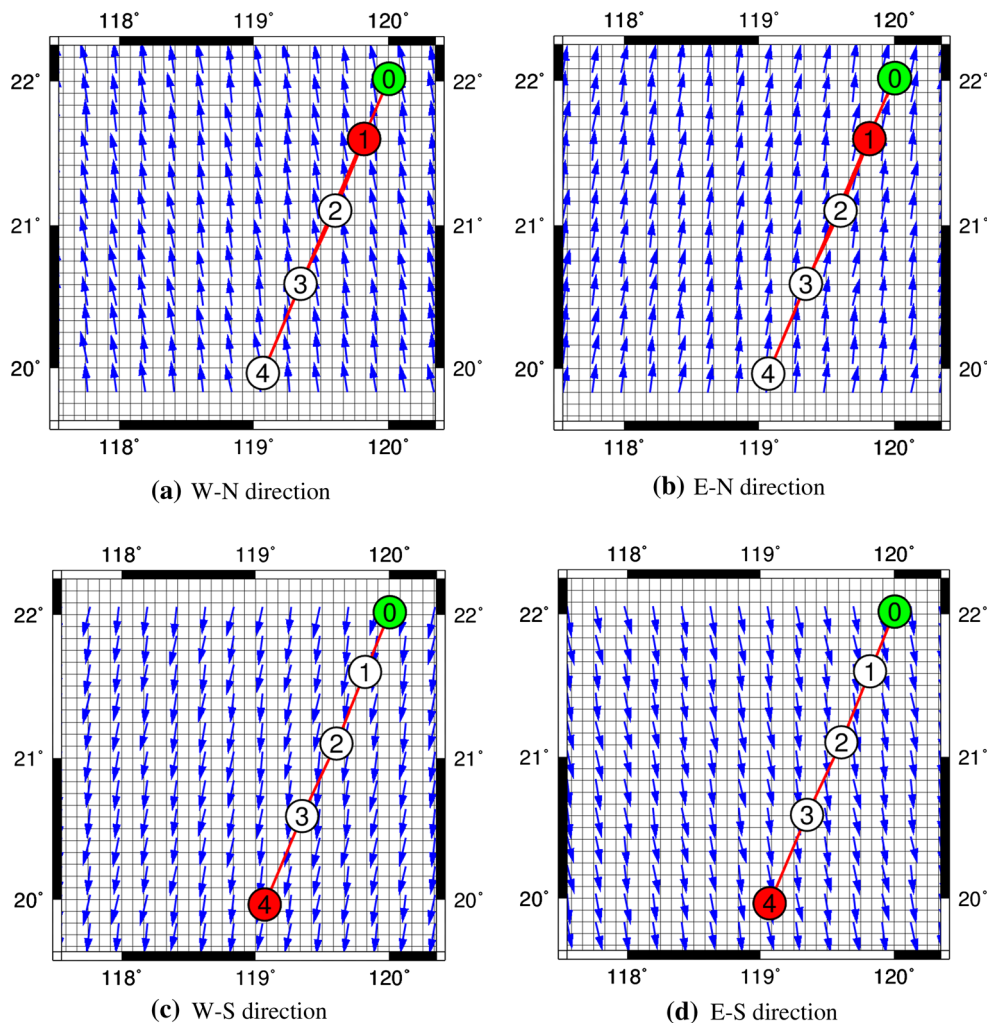


Fig. 2 A simple mission to verify the optimal path in various currents

by the red line in Fig. 1b, the solved eef is close to zero. To promote this sub-path to be a reachable one, it is possible to re-shape the effective curve by giving a smaller CS parameter. This sub-path, therefore, has a chance to be promoted as a reachable one when the CS parameter is reduced to 0.1 ($\alpha = 0.1$), as shown by the orange line in Fig. 1b. At the same time, the solved eef of this sub-path has the higher value than the previous one with $\alpha = 0.1$. Thus, the CS parameter dominates the EEF to discover a reachable path. However, determination of the appropriate CS parameter for discovery of an optimal path is a critical task. This task will be done by a routine process and described in Sect. 4.3.

3.4 Definition of optimal path in AUG path-planning problem

The goal of TSP is to find a global best solution with the shortest traveling distance. However, the shortest traveling or cruising distance is not an extreme objective to be reached in this work. As mentioned previously, the safety is the most

important concern of scientists. To verify the optimal path problem, there are 4 scenarios in a simple mission with various current directions varied in velocity are created, as shown in Fig. 2. Different from the mission, a scenario means that based on a given mission with the desired waypoints, a specific fitness function is applied in hybrid-GA with the same GA configuration to discover a path for aiding the glider cruise. These four scenarios with the same CS parameter ($\alpha = 0.1$) are created in four current directions; they are the east–northward (E–N), the east–southward (E–S), the west–southward (W–S) and the west–northward (W–N) directions. The blue arrow indicates the current direction with a velocity. The EEF is specified as the fitness function and applied in hybrid-GA with the same GA configuration to discover paths for these four scenarios. The optimal path with the maximal eef is discovered in the W–S direction, as shown in Fig. 2c; while the worst path with the minimal eef is discovered in the W–N direction, as shown in Fig. 2a. Numeric results of this simple mission are shown in Table 3. In scenarios with the W–S and E–S current directions, the path along with the DC

Table 3 Numeric results in a simple mission

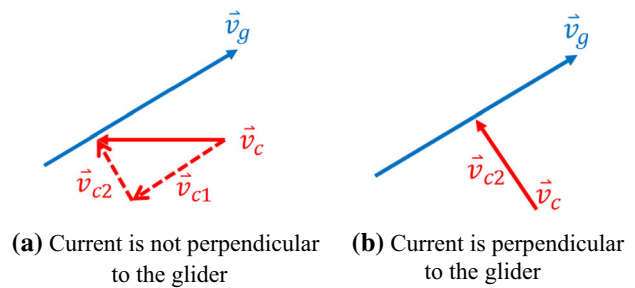
Current direction	Best fitness	Best distance (m)	Path sequence
W-N (a)	1.15	446,500	0-4-3-2-1
E-N (b)	1.30	446,500	0-4-3-2-1
W-S (c)	2.39	248,355	0-1-2-3-4
E-S (d)	2.14	248,355	0-1-2-3-4

results in the shortest cruising distance. However, in scenarios with the W-N and E-N current directions, one sub-path (from wp_0 to wp_4) confronts the UC and the paths result in the worst paths with the longest cruising distances. The cruising distance resulted in the longest distance is due to the scheme of UCA.

The path as shown in Fig. 2c is a better one with the maximal fitness than others. This path is not only an optimal path, but also a global best path. The global best path solution is able to be discovered if and only if the glider moves exactly along with the DC on each sub-path. However, this is just an example. In TSP, the global best solution with the shortest traveling distance may be found in the constant environment. However, in the real oceans, currents are not constant in a path and vary their velocity and direction all the time. That means, the global best solution may not or even never be found in variable oceans. Moreover, in the GPP, it is hard to discover a path with the shortest cruising distance and still to avoid the UC completely. An alternative, therefore, is used to make a compromise between the shortest cruising distance and exclusive of the UC. For the glider safety, the path with the minimum upstream-current sub-paths (UPs) is superior to the path with the shortest cruising distance. Thus, a new definition of the optimal path is given as “a path with the minimum UPs to approximate the minimal cruising distance in the condition that the discovered cruising distance should be less than the glider cruising range”. The EEF is developed to meet the objective of GPP that can discover the optimal path in this work.

3.5 New theorems for path reachability with upstream-current avoidance

In fact, the glider path-planning is affected deeply by current effects. The current velocity is decomposed to two velocity components \vec{v}_{c1} and \vec{v}_{c2} . \vec{v}_{c1} is the horizontal velocity component parallel with \vec{v}_g and \vec{v}_{c2} is the vertical velocity component perpendicular to \vec{v}_g , as shown in Fig. 3. The \vec{v}_{c1} will increase or decrease the glider velocity toward the next waypoint. The \vec{v}_{c2} will affect the glider heading; however, the mis-heading of the glider will be corrected by GPS signal when the glider resurfaces periodically. Thus, the perpendicular current does not affect the velocity component but the horizontal component. When currents are not perpendicular

**Fig. 3** An example of the glider motion affected by the current effects

to the glider, the current velocity affects the glider velocity and heading, as shown in Fig. 3a. When the current is perpendicular to glider, currents only change the glider heading, rather than the horizontal velocity component toward the next waypoint, as shown in Fig. 3b. In this case, low and high velocity of current actually has the same result to keep the velocity component toward the next waypoint.

In the GPP, there is a sufficient condition of reachability when the glider velocity is higher than the current velocity, namely, $\vec{v}_g > \vec{v}_c$. To consider the glider safety, a more strict condition is studied to discover the reachable path. In case of the glider velocity slightly higher than the current velocity, the difference of velocity between the glider velocity and the current velocity is small. The glider has weak capability to overcome the UC. The difference of velocity, namely the glider effective velocity \vec{v}_e , is used to set a sufficient and necessary condition. The glider effective velocity is significant to affect the reachability that the glider approaches to its destination. Afterward, there are two conditions for the reachability in the glider path-planning; the first condition is held when the glider effective velocity is higher than the current velocity (namely $\vec{v}_e > \vec{v}_c$); the second condition is held when the glider effective velocity is lower than the current velocity (namely $\vec{v}_e < \vec{v}_c$). In the first condition, a glider will be able to approach to its destination if its effective velocity is always higher than the current velocity. In other words, even in the UC case, the glider has sufficient velocity to overcome the UC. The second condition is the most important case that makes the glider avoid the UP. In this case, an angle dominating the path reachability, called the DCA, is an important angle to set the reachable condition that the path reachability should be confined to the DCA. Thus, two theorems are developed to set the path availability for the GPP when the current velocity is higher than the glider effective velocity.

Theorem 1 A reachable sub-path of the glider path-planning should be confined to DCA.

Proof In the first condition mentioned above, the DCA is unbounded when the glider velocity is higher than the current velocity. However, the second condition is the most important case we focused on. Thus, assume that current velocity (\vec{v}_c)

is greater than the glider effective velocity (\vec{v}_e). Therefore, an inequality is given by

$$|\vec{v}_e| < |\vec{v}_c| \Rightarrow \sqrt{(\vec{v}_{gx} + \vec{v}_{cx})^2 + (\vec{v}_{gy} + \vec{v}_{cy})^2} < \sqrt{(\vec{v}_{cx} + \vec{v}_{cy})^2} \tag{9}$$

because

$$\vec{v}_g = |\vec{v}_{gx}| + |\vec{v}_{gy}| = |\vec{v}_g| \cos \theta_g + |\vec{v}_g| \sin \theta_g \tag{10a}$$

and

$$\vec{v}_c = |\vec{v}_{cx}| + |\vec{v}_{cy}| = |\vec{v}_c| \cos \theta_c + |\vec{v}_c| \sin \theta_c \tag{10b}$$

Then, Eq. (9) can be modified as

$$\left(|\vec{v}_g| \cos \theta_g + |\vec{v}_c| \cos \theta_g \right)^2 + \left(|\vec{v}_g| \sin \theta_g + |\vec{v}_c| \sin \theta_c \right)^2 < \left(|\vec{v}_c| \cos \theta_c + |\vec{v}_c| \sin \theta_c \right)^2 \tag{11}$$

By squaring and subtracting the duplicates of both sides, Eq. (11) can be deduced as

$$|\vec{v}_g|^2 \left(\sin^2 \theta_g + \cos^2 \theta_g \right) + 2 |\vec{v}_g| |\vec{v}_c| \times \left(\cos \theta_g \cos \theta_c + \sin \theta_g \sin \theta_c \right) < 0 \tag{12}$$

because

$$\sin^2 \theta_g + \cos^2 \theta_g = 1 \tag{13a}$$

and

$$\cos \theta_g \cos \theta_c + \sin \theta_g \sin \theta_c = \cos (\theta_g - \theta_c) \tag{13b}$$

From Eq. (12), we have

$$|\vec{v}_g|^2 + 2 |\vec{v}_g| |\vec{v}_c| \cos (\theta_g - \theta_c) < 0 \tag{14}$$

then

$$\cos (\theta_g - \theta_c) < -\frac{|\vec{v}_g|}{2 |\vec{v}_c|} \tag{15}$$

Let $\theta_{ec} = \theta_g - \theta_c$ and $\theta'_{c_j} = \cos^{-1} \left(-\frac{|\vec{v}_g|}{2 |\vec{v}_{c_j}|} \right)$, we have a condition of the downstream-current sub-path (DP), given by

$$\theta_{ec} < \theta'_{c_j} \tag{16}$$

where θ'_{c_j} is the DCA on the j th sub-path. The effective angle θ_{ec} is an actual heading that the glider deviates its heading due to current effects. A reachable sub-path is applicable for the glider cruise if the effective angle is smaller than the DCA. Otherwise, the glider may confront the stronger currents over the glider cruising capability and the discovered sub-path may turn into an unreachable one. The DCA is useful for determination of path reachability. A reachable path should involve the minimum UPs as possible as it can. Afterward, a critical angle is found in condition of the glider velocity equivalent to the current velocity, given by

$$\theta''_c = 2\pi/3 \tag{17}$$

where θ''_c is a critical angle. The DCA is able to determine the sub-path reachability, while the critical angle is used to set the angle thresholds of the glider velocity relevant to the current velocity, given by

$$\theta'_{c_j} \leq \theta''_c, \text{ if } |\vec{v}_g| \leq |\vec{v}_{c_j}| \tag{18}$$

$$\theta'_{c_j} > \theta''_c, \text{ if } |\vec{v}_g| > |\vec{v}_{c_j}| \tag{19}$$

Equation (18) represents that the DCA never exceeds the critical angle when the glider velocity is less than or equal to the current velocity, while Eq. (19) represents that the DCA is unbounded when the glider velocity is higher than the current velocity. The composite paradigm related to the glider and current velocities is shown in Fig. 4. In case of the current velocity higher than the glider velocity, the boundary angles (BAs) of the DC should be declared as the angle constraints of the DCA. Then, BAs are derived from Theorem 1.

Theorem 2 A sub-path can be considered as a reachable one if only if the glider heading is confined to BAs.

Proof Assume that the current velocity is higher than the glider effective velocity. Thus, the angle constraints of the DC on the sub-path is given by

$$\theta'_{c1_j} = \theta_{c_j} - \frac{1}{2} \theta'_{c_j} \tag{20a}$$

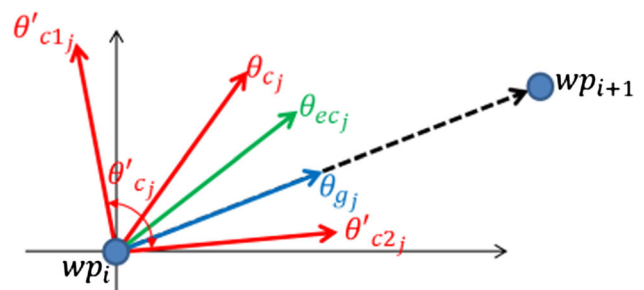


Fig. 4 Vector relations between the glider heading and current direction

$$\theta'_{c2j} = \theta_{c_j} + \frac{1}{2}\theta'_{c_j} \tag{20b}$$

where θ'_{c1j} and θ'_{c2j} are the boundary angles of the DCA on the j th sub-path. Equation 20(a) and 20(b) can be combined as

$$\theta'_{c_j} = \theta'_{c2j} - \theta'_{c1j} \tag{21}$$

The discovered sub-path can be considered as a reachable one if the effective angle is bounded by

$$\theta'_{c1j} < \theta_{ecj} < \theta'_{c2j} \tag{22}$$

because of $\theta_{ecj} = \theta_{g_j} - \theta_{c_j}$, we have

$$\theta'_{c1j} < (\theta_{g_j} - \theta_{c_j}) < \theta'_{c2j} \tag{23}$$

From Eqs. (20) to (23), we have

$$\left(2\theta_{c_j} - \frac{1}{2}\theta'_{c_j}\right) \leq \theta_{g_j} \leq \left(2\theta_{c_j} + \frac{1}{2}\theta'_{c_j}\right) \tag{24}$$

$$\check{\theta}_{c_j} \leq \theta_{g_j} \leq \hat{\theta}_{c_j}; \check{\theta}_{c_j} = \theta_{c_j} - \frac{1}{2}\theta'_{c_j}; \hat{\theta}_{c_j} = 2\theta_{c_j} + \frac{1}{2}\theta'_{c_j} \tag{25}$$

where $\check{\theta}_{c_j}$ and $\hat{\theta}_{c_j}$ are the lower and upper bound BAs to confine the glider heading on the j th reachable sub-path, respectively. The BAs are significant to describe the conditions of the reachable sub-path. Therefore, the DCA and BAs activate the important conditions to verify the path reachability for the GPP in next section.

4 Numeric results

4.1 Mission deployments

In this work, currents for the ocean-sampling missions are classified into two variations; the first variation is held when currents vary in the RRCV; the second variation is held when currents of the KCET are generated from the ocean prediction model. In the first current variation, four missions (Mission A–D) with various waypoints are created to simulate the glider path-planning in four current directions. Four current directions are the E–N, the E–S, the W–S and the W–N directions. Thus, total 112 scenarios involving 7 fitness functions are presented in these four missions with four current directions. In the second current variation, three missions (KCET Mission A–C) with various waypoints are created to simulate the glider path-planning in the KCET. Thus, total 21 scenarios involving 7 fitness functions are presented in three KCET missions. Each scenario in a mission is given with a specific fitness function but the same GA configuration to discover a path. Waypoint distributions of all missions are shown in

Table 4 Waypoint distributions

Mission	A	B	C	D	KCET-A	KCET-B	KCET C
Waypoints	9	16	32	48	10	35	48

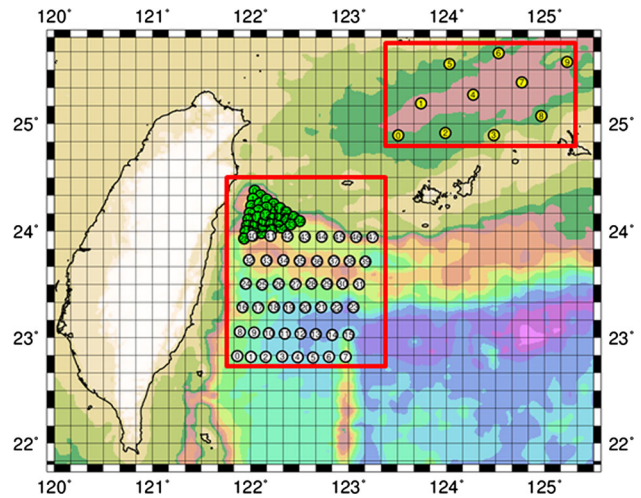


Fig. 5 Graphic waypoint distributions of three missions in the KCET

Table 4. Missions from A to D are created by random distribution, while three KCET Missions are created by regular distribution in the west Pacific near Taiwan, as shown in Fig. 5.

4.2 Current variations

In this work, the glider is approached to the GPP in short inter-waypoint distances such as the Kuroshio current with less than 100 km. In conditions of the short inter-waypoint distance, the current glider travels in a day between successive waypoints. There is a good method to densely deploy dozens of waypoints to imitate the long cruising distance in a mission and to reduce the current variation effect on each sub-path. Thus, the offshore current variation can be considered as slight in both magnitude and direction that can be ignorable in the short inter-waypoint distance. However, the current variation on the next sub-path is dissimilar to the previous one. In the first current variation of the RRCV, the current velocity varies randomly in the zonal (horizontal, U) and meridional (vertical, V) directions, given by

$$U_j = \begin{cases} + \left[U - \frac{U_r}{2} + \text{Rnd}(U_r) \right], & \text{eastward} \\ - \left[U - \frac{U_r}{2} + \text{Rnd}(U_r) \right], & \text{westward} \end{cases} \tag{26}$$

$$V_j = \begin{cases} + \left[V - \frac{V_r}{2} + \text{Rnd}(V_r) \right], & \text{northward} \\ - \left[V - \frac{V_r}{2} + \text{Rnd}(V_r) \right], & \text{southward} \end{cases} \tag{27}$$

where U_j and V_j are the restricted random current velocities on the j th sub-path. U and V are the user-defined current

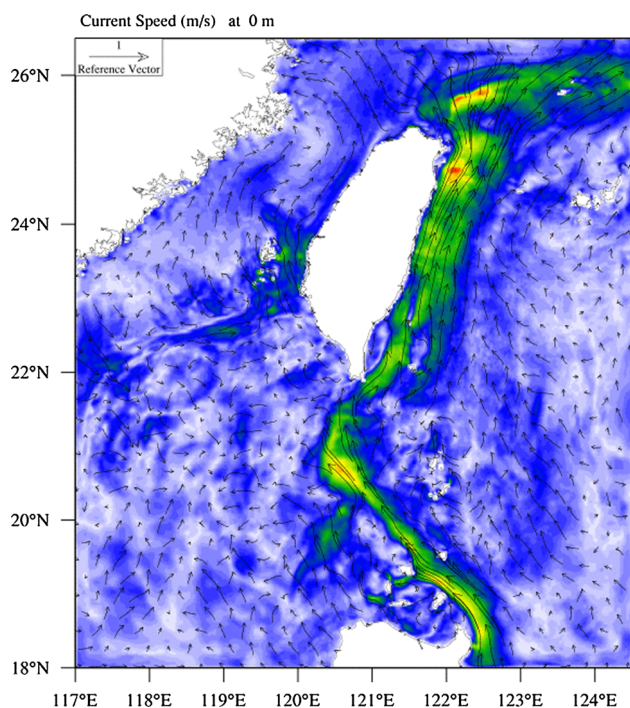


Fig. 6 Kuroshio current of east of Taiwan generated by TOPS¹

velocities. U_r and V_r are the variable ranges of the current velocities. $Rnd()$ is a random function. For example, assume that the user-defined current velocity is 0.3 m/s and the variable ranges are 0.1 m/s, then currents are varied between 0.25 and 0.35 m/s. In the first variation of the RRCV, the current velocities are lower than or equal to the glider nominal velocity.

To create more real-ocean simulation and imitate the near-real current variations in the second current variation of the KCET, a Princeton Ocean Model-based offshore Taiwan Ocean Prediction Systems (TOPS)¹ is introduced to generate the KCET data, as shown in Fig. 6. The KCET presents the northward-like direction. The Kuroshio current is one of the major currents in the world’s oceans that occupies only a small fraction of North Pacific Ocean: a thin narrow band less than 100 km in width and about 1 km at maximum depth running for 3000 km along the western edge of the Pacific between the Philippines and the east coast of Japan (Barkley 1970). To simulate more real KCET, the KTW (Kuroshio Tropical Water) of paper (Mensah et al. 2014) is studied on the correction of current velocity. This paper provided long-duration observation in the KTW and showed actual and simulated salinity maximum from 18.75 to 24°N, as shown in Fig. 7. The black dotted-line displays the evolutions of the current velocity at the level of KTW salinity maximum. Thus, the current variations of KCET are between 0.52 and 0.58 m/s. In the second variation of the KCET, the

¹ <http://tops.tori.org.tw>.

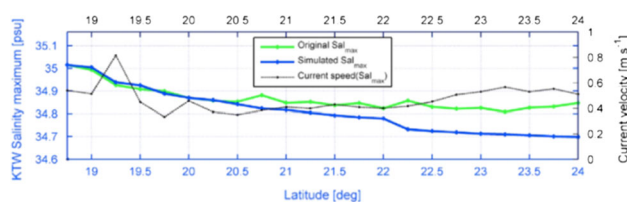


Fig. 7 Evolutions of Kuroshio Tropical Water (Mensah et al. 2014)

Table 5 Appropriate CS parameters for all missions

Mission	Waypoints	E–N	E–S	W–S	W–N
A	9	0.5	0.5	0.4	0.4
B	16	0.6	0.6	0.1	0.5
C	32	0.5	0.6	0.7	0.2
D	48	0.2	0.5	0.4	0.2
KCET-A	10	0.4			
KCET-B	35	1.0			
KCET-C	48	0.7			

current velocities are higher than the glider nominal velocity (0.35 m/s).

4.3 Determination of curve shaping parameters

As the mentioned above, the CS parameter of the EEF is used to diverse the path reachability. To determine the appropriate CS parameters for each mission, a routine process is adopted to verify the performances of the various CS parameters. Different CS parameter involved in a mission resulted in change of the path sequence and the dissimilar cruising distance as well as the number of UPs. However, the detailed results of routine process create a large table and only the accepted CS parameters for all missions are concluded, as shown in Table 5.

4.4 Evaluation criterions

To make fair comparisons with the EEF, the compared 6 state-of-the-art fitness functions are briefly reviewed in Sect. 2.1; they are effective speed (ES) (Shih et al. 2012), energy cost (EC) (Alvarez et al. 2004), reaching cost (RC) (Fernandez-Perdomo et al. 2011), hybrid search (HS) (Pêtrès et al. 2007), actual travel time (ATT) (Soullignac 2011), and effective function (EF) (Shih et al. 2014). All fitness functions are applied in hybrid-GA with the same GA configuration in a mission to solve the GPP. The fitness functions such as the EEF, ES and EF are seeking the maximum fitness, while others are seeking the minimum fitness. All fitness functions evaluated the performances of a path in reachability and efficiency as well as the stability of convergent solution. Reachability is evaluated by the number of UPs by Eq.

(25), while efficiency is evaluated by the cruising distance by Eq. (6) and the distance overhead. The number of UPs is increased when the glider heading is over the BAs. The distance overhead is the cruising distance ratio of the compared fitness function and the EEF, given by

$$O_{\text{dist}} = \frac{d_{\text{best}}^{\text{other}}}{d_{\text{best}}^{\text{EEF}}} \times 100 \% \quad (28)$$

where O_{dist} is the distance overhead; $d_{\text{best}}^{\text{other}}$ and $d_{\text{best}}^{\text{EEF}}$ are the cruising distances discovered by compared fitness function and the EEF, respectively. In evaluation of the path stability, the coefficient of variation (CV) as the ratio of standard deviation and mean is used to evaluate the convergent solution, given by

$$\text{CV} = \frac{\sigma(d_{\text{best}})}{\mu(d_{\text{best}})} \times 100 \% \quad (29)$$

where d_{best} is the best efficiency of the cruising distance discovered by the fitness function in a path. σ and μ are the functions of standard deviation and mean, respectively. The CV is a meaningful tool that analyzes the solution stability, and compares the variability of two or more samples of data from different variables or from the same variables when the means are very different (Lovie 2005). Lower CV means the more stable or convergent solution we have; however, higher CV leads to path solution variation or divergence from the optima.

4.5 Numeric results of AUG path-planning in restricted random current variations

Each time the RRCV generates different current variations for four missions (Mission A–D) and currents vary in both

velocity and direction. Numeric results of Mission A are presented in Table 6. The EEF discovers the optimal paths with the shorter cruising distance than others, except for EC in the W–S current direction. In this case, EC is a good fitness function to shorten the cruising distance. However, to inspect the UPs, as the column of UPs, the EEF discovers the minimum UPs but a bit long cruising distance around 5 % distance overhead more than EC does. EC discovers the most 7 UPs same as ATT. In other words, the EEF tries to discover a path following the DC on the way to the target as possible as it can. As mentioned previously, it is hard to discover a path without the UC completely in the variable currents. There are only 2 UPs discovered by the EEF; that means, path reachability of the EEF is better than other fitness functions do. The minimal and maximal distance overheads are 95 and 161 % discovered by EC in the W–S current direction and ES in the E–N current direction, respectively.

In the most ocean-sampling missions, the glider travels continuously over periods of weeks, even months (Leonard et al. 2007) and could have dozens of waypoints in a mission. To simulate more complex ocean-sampling mission, Mission B with 16 waypoints is created. Numeric results of Mission B are presented in Table 7. The EEF discovers the optimal paths with the minimum UPs and the shorter cruising distance than others do. The minimal and maximal distance overheads are 100 and 166 % discovered by EF and RC in the E–S current direction, respectively.

Furthermore, additional two missions are created. Mission C extends Mission B to 32 waypoints, while Mission D extends Mission C to 48 waypoints. Numeric results of these two missions are shown in Tables 8 and 9. In Mission C and D, the EEF discovers the optimal paths with the minimum UPs and the shortest cruising distance to all scenarios. The minimal and maximal distance overheads of Mission C are 100 and 209 % discovered by HS in the W–N current direction and ATT in the E–S current direction, respectively. The

Table 6 Performance comparisons in Mission A

Fit. func.	E–N			E–S			W–S			W–N		
	UPs	Dist. (km)	O_{dist} (%)	UPs	Dist. (km)	O_{dist} (%)	UPs	Dist. (km)	O_{dist} (%)	UPs	Dist. (km)	O_{dist} (%)
ES (Shih et al. 2012)	6	89.50	161	5	70.03	121	6	74.54	127	6	63.82	105
EC (Alvarez et al. 2004)	7	58.50	105	3	57.74	100	7	55.74	95	3	60.70	100
RC (Fernandez-Perdomo et al. 2011)	6	78.25	140	6	67.98	118	4	74.28	127	7	70.01	115
HS (Pêtrès et al. 2007)	7	74.14	133	5	74.14	128	4	74.14	127	6	74.13	122
ATT (Soullignac 2011)	5	70.60	127	6	75.72	131	6	76.58	131	7	64.05	106
EF (Shih et al. 2014)	3	55.74	100	4	58.42	101	2	58.50	100	3	60.70	100
EEF	3	55.74	100	3	57.74	100	2	58.50	100	3	60.70	100

Table 7 Performance comparisons in Mission B

Fit. func.	E–N			E–S			W–S			W–N		
	UPs	Dist. (km)	O_{dist} (%)	UPs	Dist. (km)	O_{dist} (%)	UPs	Dist. (km)	O_{dist} (%)	UPs	Dist. (km)	O_{dist} (%)
ES (Shih et al. 2012)	12	1327	125	9	1180	139	11	1455	157	10	1109	106
EC (Alvarez et al. 2004)	15	1067	101	4	1044	123	13	1217	131	5	1172	112
RC (Fernandez-Perdomo et al. 2011)	13	1389	131	8	1410	166	10	1145	123	9	1126	108
HS (Pêtrès et al. 2007)	12	1157	109	8	1159	136	10	1159	125	11	1157	111
ATT (Soulignac 2011)	12	1140	108	9	1276	150	10	1432	154	11	1100	105
EF (Shih et al. 2014)	6	1088	103	3	850	100	5	1026	111	5	1052	101
EEF	6	1060	100	3	850	100	5	927	100	5	1044	100

Table 8 Performance comparisons in Mission C

Fit. func.	E–N			E–S			W–S			W–N		
	UPs	Dist. (km)	O_{dist} (%)	UPs	Dist. (km)	O_{dist} (%)	UPs	Dist. (km)	O_{dist} (%)	UPs	Dist. (km)	O_{dist} (%)
ES (Shih et al. 2012)	27	5511	151	18	5423	155	22	4299	124	19	5056	119
EC (Alvarez et al. 2004)	27	3894	107	7	4627	132	29	4551	131	8	4761	112
RC (Fernandez-Perdomo et al. 2011)	27	5940	162	13	5488	156	23	5710	165	18	5694	134
HS (Pêtrès et al. 2007)	24	4379	120	13	4355	124	23	4505	130	23	4268	100
ATT (Soulignac 2011)	27	5101	140	16	7321	209	25	5462	158	19	5512	129
EF (Shih et al. 2014)	16	4594	126	7	4007	114	15	3611	104	10	4824	113
EEF	13	3656	100	6	3509	100	15	3464	100	8	4262	100

Table 9 Performance comparisons in Mission D

Fit. func.	E–N			E–S			W–S			W–N		
	UPs	Dist. (km)	O_{dist} (%)	UPs	Dist. (km)	O_{dist} (%)	UPs	Dist. (km)	O_{dist} (%)	UPs	Dist. (km)	O_{dist} (%)
ES (Shih et al. 2012)	34	10088	149	30	10613	151	35	9197	131	34	10895	154
EC (Alvarez et al. 2004)	39	8114	120	13	7952	113	37	8837	126	16	8208	116
RC (Fernandez-Perdomo et al. 2011)	32	9816	145	33	9537	136	31	9926	141	30	9092	129
HS (Pêtrès et al. 2007)	36	7134	105	27	7720	110	33	7967	114	36	7852	111
ATT (Soulignac 2011)	37	10035	148	29	9886	141	28	9737	139	35	10488	149
EF (Shih et al. 2014)	19	8159	120	15	7250	103	16	7138	102	21	7445	105
EEF	19	6784	100	12	7029	100	15	7020	100	16	7061	100

Table 10 Path sequences in Mission A–D

Mission	Dir.	Path sequence
A	E–N	0-2-5-4-3-6-7-8-1
	E–S	0-3-8-1-2-7-6-5-4
	W–S	0-5-2-3-4-1-8-7-6
	W–N	0-8-3-2-1-4-5-6-7
B	E–N	0-14-13-12-9-5-15-10-7-8-4-1-11-6-3-2
	E–S	0-2-3-7-13-9-8-6-15-11-5-1-4-10-12-14
	W–S	0-1-4-8-13-14-7-10-15-12-5-9-2-3-6-11
	W–N	0-13-7-3-4-11-2-1-5-14-12-10-15-6-8-9
C	E–N	0-11-15-10-7-8-4-1-22-19-12-13-16-18-30-28-27-6-3-2-21-25-26-14-20-17-23-9-5-31-29-24
	E–S	0-4-3-16-18-23-24-25-27-5-1-11-10-12-17-19-26-9-2-7-14-29-28-8-6-15-13-20-21-22-31-30
	W–S	0-1-5-9-16-13-14-7-12-25-24-23-19-21-3-6-18-17-20-8-27-28-30-22-2-4-10-15-11-26-29-31
	W–N	0-31-14-2-1-5-27-25-19-18-17-16-7-3-4-28-29-23-12-30-22-20-10-11-6-9-26-24-21-13-15-8
D	E–N	0-36-37-41-43-45-12-7-16-34-29-28-13-17-32-46-9-8-5-3-31-27-26-14-20-18-30-24-47-11-15-10-22-25-6-1-21-19-23-33-39-4-2-35-38-40-42-44
	E–S	0-7-16-17-22-23-25-27-39-40-26-9-8-6-15-14-24-28-4-10-12-18-20-21-41-37-33-29-30-5-3-13-19-31-44-1-2-35-34-32-45-43-42-46-11-36-38-47
	W–S	0-1-6-11-46-39-32-24-29-31-35-16-10-47-23-19-3-8-44-43-41-36-20-21-42-26-27-28-30-18-17-14-45-37-2-4-12-25-22-13-5-9-40-38-33-34-7-15
	W–N	0-27-23-34-36-43-20-17-7-3-28-24-18-35-2-1-25-33-21-13-12-5-40-39-37-14-15-6-8-11-30-31-22-47-46-42-44-45-29-19-16-10-4-9-26-32-38-41

minimal and maximal distance overheads of Mission D are 102 and 154 % discovered by EF in the W–S current direction and ES in the W–N current direction, respectively. The path sequences discovered by the EEF in Mission A–D are presented in Table 10.

Numeric results of four missions with the RRCV show that the EEF is able to reach the expected objective of the optimal path in the GPP. The EEF not only develops as a good fitness function to evaluate the fittest path but also optimizes the path with the minimum UPs to approximate the minimal cruising distance. Besides, with the growing waypoints, the EEF indeed exhibits outstanding performances in terms of path reachability and efficiency. In the GPP, a path with the shortest cruising distance may have more UPs on the way to the target. A path-planning approach should detour round UP

and shorten the cruising distance to approximate the minimal cruising distance in a path.

In fact, the cruising distance of a glider is essentially concerned with the cruising capability and safety in the oceans. A path-planning approach should be able to advice scientists whether the estimative cruising distance goes beyond the glider enduring range or not. The glider has limitation of the cruising range due to internal battery capacity. For instance, the commercial gliders such as Slocum (Webb et al. 2001), Spray (Sherman et al. 2001) and Seaglider (Rudnick et al. 2004), have maximum cruising ranges in 4000, 6000 and 4600 km, respectively. In case of Mission D, the shortest cruising distances discovered by the EEF exceeds the enduring range that the commercial gliders can do. This is an alert to notify scientists that it is better to reduce the amount of waypoints or to deploy multiple gliders to collaborate in a mission. In consideration of the glider cruising distance, consequently the KCET missions are created in the smaller areas than Mission D.

4.6 Numeric results of AUG path-planning in near-real oceans

In contrast to the RRCV, the KCET missions with the higher current velocity are created to simulate the glider path-planning in near-real oceans. Numeric results are presented in Table 11. The EEF discovers the paths with the minimum UPs to approximate minimal cruising distances better than others do. However, there is a distinctive case of the KCET Mission B to be discussed honestly. In this case, EF is a good fitness function to discover the shorter cruising distance than the EEF does; however, the UPs are more than the EEF does. That means, the EEF detours around the UC so that it can reduce UPs. In this case, the path discovered by the EEF devotes additional 16 km around 4 % distance overhead. For the glider safety, it is worth to sacrifice a bit distance to avoid the UC. With the growing waypoints up to 48 of KCET Mission C, the EEF indeed discovers the optimal path. The maximal distance overheads are discovered by RC (151 %) in KCET Mission A, ATT (134 %) in KCET Mission B, and RC (143 %) in KCET Mission C.

Afterward, the CV is used to measure the stability of the data expressed in percentage. The stability of the solved path is highly dependent on the optimization algorithm. An efficient optimization algorithm is able to lead the solution to convergence quickly. A hybrid-GA is designed as the optimization algorithm to solve the GPP in this work. The stability in all scenarios of KCET missions are analyzed by the CV, as shown in Table 12. As the CV results, all scenarios are maintained in the lower values. That means, the proposed hybrid-GA is an efficient optimization algorithm that is able to converge the solution in rapidity. Thus, a partial success of the proposed path-planning approach to the GPP

Table 11 Performance comparisons in KCET missions

Fit. func.	KCET Mission A			KCET Mission B			KCET Mission C		
	Dist. (km)	O_{dist} (%)	UPs	Dist. (km)	O_{dist} (%)	UPs	Dist. (km)	O_{dist} (%)	UPs
ES (Shih et al. 2012)	702	124	8	736	124	27	3262	138	41
EC (Alvarez et al. 2004)	765	136	7	632	106	29	2887	122	39
RC (Fernandez-Perdomo et al. 2011)	854	151	8	757	127	26	3384	143	37
HS (Pêtrès et al. 2007)	675	120	9	617	104	29	2564	109	38
ATT (Soulignac 2011)	769	136	8	800	134	26	3106	132	35
EF (Shih et al. 2014)	564	100	5	579	97	15	2431	103	18
EEF	564	100	5	595	100	13	2362	100	18

Table 12 Stability analyses of convergent path solution in KCET Missions

Mission Fit. func.	KCET Mission A			KCET Mission B			KCET Mission C		
	μ	σ	CV	μ	σ	CV	μ	σ	CV
ES (Shih et al. 2012)	657	71	10.82	740	23	3.18	3150	145	4.61
EC (Alvarez et al. 2004)	748	48	6.39	594	40	6.68	2927	70	2.38
RC (Fernandez-Perdomo et al. 2011)	854	0	0.00	801	57	7.15	3373	29	0.86
HS (Pêtrès et al. 2007)	675	0	0.00	643	37	5.70	2585	74	2.85
ATT (Soulignac 2011)	699	80	11.45	784	11	1.40	3139	190	6.04
EF (Shih et al. 2014)	565	3	0.57	573	16	2.76	2500	125	5.00
EEF	567	3	0.57	618	35	5.67	2562	82	3.20

μ mean in km, σ standard deviation in km, CV coefficient of variation in %

is ascribed to the rapidly convergent hybrid-GA. Finally, the graphic paths of the KCET missions discovered by the EEF are shown in Fig. 8.

5 Conclusions

In computational intelligence science, most state-of-the-art optimization algorithms create efficient approaches to discover the global best path solutions in particular research fields. Development of a fitness function for the path-planning problem is the key that obviously influences the performance and stability of path solution, especially in the environment variability. Because of variable oceans, currents severely affect the glider path-planning in terms of efficiency and reachability. Discovery of a global optimal path solution with the minimum UPs and with the shortest cruising distance becomes a difficult task. However, for the glider safety, an alternative is to compromise the trade-off between reachability and efficiency. A condition of the optimal path with the minimum UPs to approximate the minimal cruising distance for solving the GPP is, therefore, defined in this work.

To solve the GPP, one of the objectives in this work is to develop a new fitness function that is able to discover an opti-

mal path and to benefit the path reachability and efficiency for glider ocean-sampling missions in real oceans. The proposed EEF considers the characteristics of not only cruising distance but also the relations between the glider motion and current effects so that is able to discover an optimal path for real applications. The benefits of reachability and efficiency are realized by exponential combination. Moreover, the scheme of UCA is enabled when the CS parameter is given a positive non-zero value between 0 and 1. Various CS parameters shape the effective curve accordingly and reorganize the path sequences obviously to excite the diversity of path reachability. To verify the DC on a path, new theorems are, therefore, developed to set the conditions for the scheme of UCA.

Prior to the simulations, a simple mission is used to verify that the global best optimal path solution can be found only in a specific situation. Afterward, two current variations are created to simulate the glider ocean-sampling missions with total 133 scenarios. Firstly, 112 scenarios are created to verify that the proposed EEF is able to discover the optimal paths in the condition of the RRCV. Secondly, 21 scenarios are created to validate that the EEF discovers the optimal paths in the condition of the KCET. Two special scenarios solved by the compared fitness functions discover the better cruising distances than the EEF does. However, the path

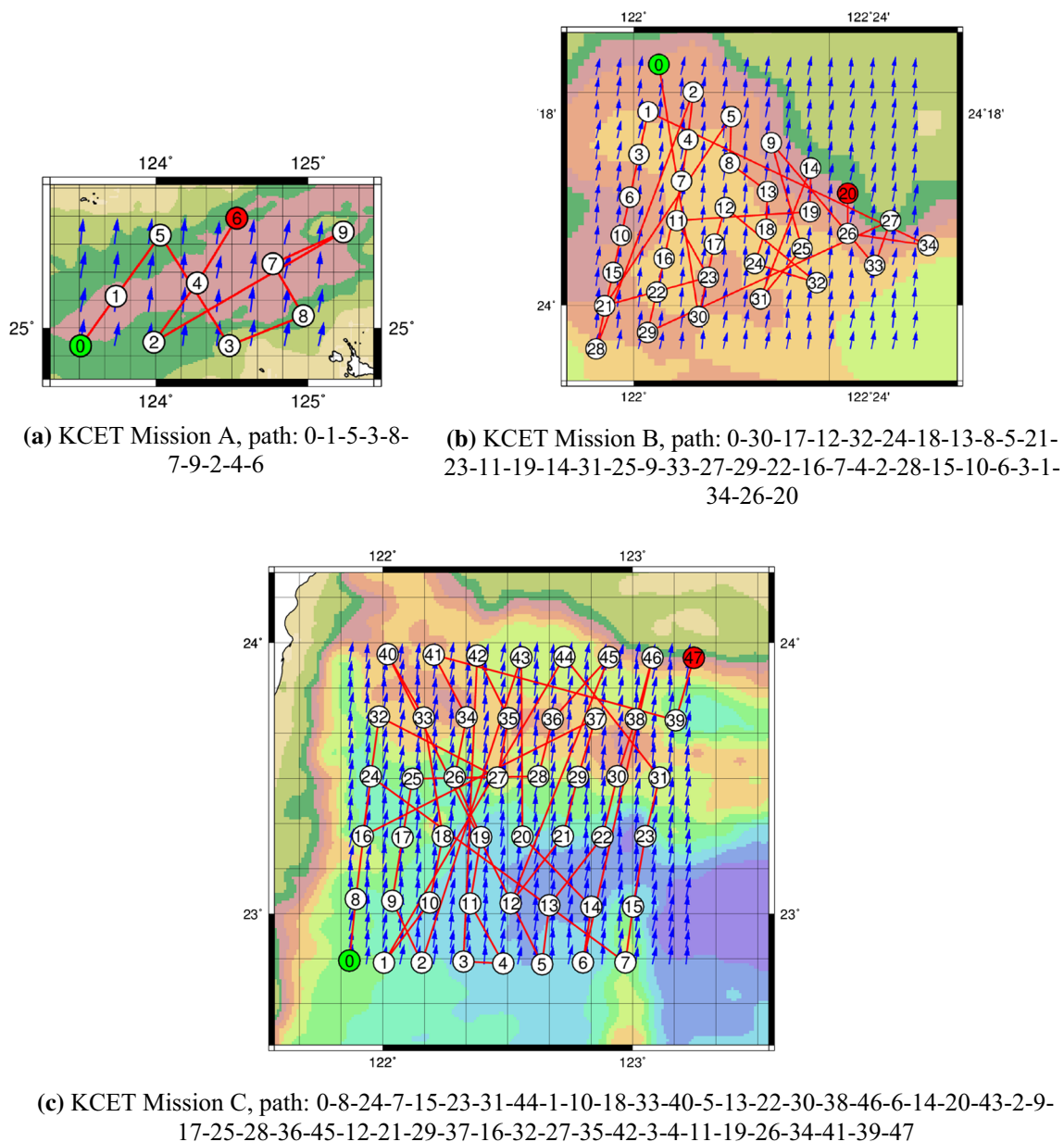


Fig. 8 Graphic paths discovered by EEF in KCET Missions

with the shortest cruising distance is not more important than the path with the minimum UPs because the glider safety is of most concern of scientists. Thus, in the GPP, the optimal path should be benefited the maximum reachability to approximate the maximum efficiency.

Numeric results show that the proposed EEF can discover the optimal path with the minimum UPs to approximate the minimal cruising distance. In point of reachability, the proposed EEF minimizes the UPs. The maximum decrements of UPs are 22 (EC) and 23 (ES) in Mission D with the W-S current direction and in KCET Mission C, respectively. In point of efficiency, the proposed EEF shortens the cruis-

ing distance to approximate the minimal cruising distance. The maximum decrements of distance overheads are 109 % (ATT) and 51 % (RC) in Mission C with the E-S current direction and in KCET Mission A, respectively. Finally, the stability of convergent solution in all scenarios of KCET missions is verified by the CV. The results show that hybrid-GA is able to maintain a low CV to lead the path solution to stability. The proposed EEF applied in hybrid-GA is developed as a premium path-planning approach to the glider ocean-sampling mission. Thus, this work contributes a path-planning approach with the UCA to the glider path-planning for solving the GPP in variable oceans.

Acknowledgements This research has been financially supported in part by the MOST ROC (Taiwan) under Grants “MOST104-2221-E-151-007”. The financial support is gratefully appreciated. The authors would also like to thank Dr. Yih Yang and Dr. Jian-Ming Liaw at Taiwan Ocean Research Institute, National Applied Research Laboratories for providing the relative support of the Kuroshio Current simulation.

Compliance with ethical standards

Conflict of interest All authors declare that they have no conflict of interest.

References

- Aghababa MP (2012) 3D path planning for underwater vehicles using five evolutionary optimization algorithms avoiding static and energetic obstacles. *Appl Ocean Res*. doi:[10.1016/j.apor.2012.06.002](https://doi.org/10.1016/j.apor.2012.06.002)
- Ahmed ZH (2010) Genetic algorithm for the traveling salesman problem using sequential constructive crossover operator. *Int J Biom Bioinform* 3(6):96–105
- Ahmed F, Deb K (2013) Multi-objective optimal path planning using elitist non-dominated sorting genetic algorithms. *Soft Comput*. doi:[10.1007/s00500-012-0964-8](https://doi.org/10.1007/s00500-012-0964-8)
- Albayrak M, Allahverdi N (2011) Development a new mutation operator to solve the Traveling Salesman Problem by aid of Genetic Algorithms. *Expert Syst Appl*. doi:[10.1016/j.eswa.2010.07.006](https://doi.org/10.1016/j.eswa.2010.07.006)
- Alcázar V, Veloso M, Borrajo D (2011) Adapting a rapidly-exploring random tree for automated planning. In: Proceedings of the fourth international symposium on combinatorial Search (SoCS-2011), pp 1–9
- Alvarez A, Caiti A, Onken R (2004) Evolutionary path planning for autonomous underwater vehicles in a variable ocean. *IEEE J Oceanic Eng*. doi:[10.1109/JOE.2004.827837](https://doi.org/10.1109/JOE.2004.827837)
- Barkley RA (1970) The Kuroshio current. *Sci J* 6:54–60
- Bhadoria A, Singh RK (2014) Optimized angular a star algorithm for global path search based on neighbor node evaluation. *Int J Intell Syst Appl (IJISA)*. doi:[10.5815/ijisa](https://doi.org/10.5815/ijisa)
- Castillo O, Trujillo L, Melin P (2007) Multiple objective genetic algorithms for path-planning optimization in autonomous mobile robots. *Soft Comput*. doi:[10.1007/s00500-006-0068-4](https://doi.org/10.1007/s00500-006-0068-4)
- Clifton M, Paul G, Kwok N, Dikai L, Wang DL (2008) Evaluating performance of multiple RRTs. In: *Mechronic and embedded systems and application*, pp 564–569. doi:[10.1109/MESA.2008.4735749](https://doi.org/10.1109/MESA.2008.4735749)
- Donald B, Xavier P, Canny J, Reif J (1993) Kinodynamic motion planning. *J ACM*. doi:[10.1145/174147.174150](https://doi.org/10.1145/174147.174150)
- Fernandez-Perdomo E et al (2010) Path planning for gliders using regional ocean models: application of Pinzón path planner with the ESEOAT model and the RU27 trans-Atlantic flight data. In: Proceedings of IEEE OCEANS, pp 1–10. doi:[10.1109/OCEANSSYD.2010.5603684](https://doi.org/10.1109/OCEANSSYD.2010.5603684)
- Fernandez-Perdomo E, Cabrera-Gamez J, Hernandez-Sosa D, Isern-Gonzalez J, Dominguez-Brito AC, Prieto-Maranon V, Ramos AG (2011) Adaptive bearing sampling for a constant-time surfacing A* path planning algorithm for gliders. In: Proceedings of IEEE international conference on robotics and automation (ICRA). doi:[10.1109/ICRA.2011.5980137](https://doi.org/10.1109/ICRA.2011.5980137)
- Groba C, Sartal A, Vázquez XH (2015) Solving the dynamic traveling salesman problem using a genetic algorithm with trajectory prediction: An application to fish aggregating devices. *Comput Oper*. doi:[10.1016/j.cor.2014.10.012](https://doi.org/10.1016/j.cor.2014.10.012)
- Hart PE, Nilsson NJ, Raphael B (1968) A formal basis for the heuristic determination of minimum cost paths. *IEEE Trans Syst Sci Cybern* 4:100–107. doi:[10.1109/TSSC.1968.300136](https://doi.org/10.1109/TSSC.1968.300136)
- Holland JH (1984) Genetic algorithms and adaptation. In: *Adaptive control of ill-defined systems*. Springer US, Boston, pp 317–333. doi:[10.1007/978-1-4684-8941-5_21](https://doi.org/10.1007/978-1-4684-8941-5_21)
- Hong TP, Huang KY, Lin WY (2002) Applying genetic algorithms to game search trees. *Soft Comput*. doi:[10.1007/s005000100154](https://doi.org/10.1007/s005000100154)
- Larrañaga P, Kuijpers CMH, Murga RH, Inza I, Dizdarevic S (1999) Genetic algorithms for the travelling salesman problem: a review of representations and operators. *Artif Intell*. doi:[10.1023/a:1006529012972](https://doi.org/10.1023/a:1006529012972)
- LaValle SM, Kuffner JJ Jr (2000) Rapidly-exploring random trees: progress and prospects. In: *Algorithmic and computational robotics: new directions: the fourth workshop on the algorithmic foundations of robotics*, pp 293–308
- LaValle SM (2006) Motion planning. In: *Planning algorithms*, 1st edn. Cambridge University Press, Cambridge, pp 79–80
- Leonard NE, Paley DA, Lekien F, Sepulchre R, Fratantoni DM, Davis RE (2007) Collective motion, sensor networks, and ocean sampling. *Proc IEEE* 95:48–74. doi:[10.1109/JPROC.2006.887295](https://doi.org/10.1109/JPROC.2006.887295)
- Lovie P (2005) Coefficient of variation. In: *Encyclopedia of statistics in behavioral science*. John Wiley & Sons, Ltd. doi:[10.1002/0470013192.bsa107](https://doi.org/10.1002/0470013192.bsa107)
- Majumdar J, Bhunia AK (2011) Genetic algorithm for asymmetric traveling salesman problem with imprecise travel times. *J Comput Appl Math*. doi:[10.1016/j.cam.2010.12.027](https://doi.org/10.1016/j.cam.2010.12.027)
- Mensah V, Jan S, Chiou M-D, Kuo TH, Lien R-C (2014) Evolution of the Kuroshio Tropical Water from the Luzon Strait to the east of Taiwan. *Deep-Sea Res*. doi:[10.1016/j.dsr.2014.01.005](https://doi.org/10.1016/j.dsr.2014.01.005)
- Moura A, Rijo R, Silva P, Crespo S (2010) A multi-objective genetic algorithm applied to autonomous underwater vehicles for sewage outfall plume dispersion observations. *Appl Soft Comput*. doi:[10.1016/j.asoc.2010.05.009](https://doi.org/10.1016/j.asoc.2010.05.009)
- Nagata Y, Soler D (2012) A new genetic algorithm for the asymmetric traveling salesman problem. *Expert Syst Appl*. doi:[10.1016/j.eswa.2012.02.029](https://doi.org/10.1016/j.eswa.2012.02.029)
- NIMA (2002) Calculations and conversions. In: *The American practical navigator: bowditch*, 2nd edn. Paradise Cay Publications, National Imagery and Mapping Agency, pp 331–332
- Pêtrès C, Pailhas Y, Patron P, Petillot Y, Evans J, Lane D (2007) Path planning for autonomous underwater vehicles. *IEEE T Robot*. doi:[10.1109/tro.2007.895057](https://doi.org/10.1109/tro.2007.895057)
- Rudnick DL, Davis RE, Eriksen CC, Fratantoni DM, Perry MJ (2004) Underwater gliders for ocean research. *Mar Technol Soc J* 38(2):73–84
- Schrijver A (2005) On the history of combinatorial optimization. In: *Handbooks in operations research and management science*, vol 12. Elsevier, Amsterdam, pp 1–68. doi:[10.1016/S0927-0507\(05\)12001-5](https://doi.org/10.1016/S0927-0507(05)12001-5)
- Sherman J, Davis R, Owens WB, Valdes J (2001) The autonomous underwater glider “Spray”. *IEEE J Oceanic Eng* 26(4):437–446. doi:[10.1109/48.972076](https://doi.org/10.1109/48.972076)
- Shih C-C, Horng M-F, Pan J-S (2012) 3-D adaptive bearing sampling for AUG route planning in extensible ocean model. In: Proceedings of 14th conference on undersea technology (CUST 2012), Kaohsiung, Taiwan (R.O.C), pp 71–84
- Shih C-C, Yang Y, Horng M-F, Pan T-S, Pan J-S (2014) An effective approach to genetic path planning for autonomous underwater glider in a variable ocean. In: Proceedings of international forum on systems and mechatronics (IFSM2014), Tainan, Taiwan (R.O.C), pp 1–6
- Skiena SS (2008) Graph problems: polynomial-time. In: *The algorithm design manual*, 2nd edn. Springer-Verlag, London, pp 495–496. doi:[10.1007/978-1-84800-070-4](https://doi.org/10.1007/978-1-84800-070-4)

- Soullignac M (2011) Feasible and optimal path planning in strong current fields. *IEEE T Robot*. doi:[10.1109/tro.2010.2085790](https://doi.org/10.1109/tro.2010.2085790)
- Spong MW, Vidyasagar M (2008) Velocity kinematics-the manipulator Jacobian. In: *Robot dynamics and control*. Wiley India Pvt. Limited, pp 99–100
- Wang Y (2014) The hybrid genetic algorithm with two local optimization strategies for traveling salesman problem. *Comput Ind Eng*. doi:[10.1016/j.cie.2014.01.015](https://doi.org/10.1016/j.cie.2014.01.015)
- Webb DC, Simonetti PJ, Jones CP (2001) SLOCUM: an underwater glider propelled by environmental energy. *IEEE J Oceanic Eng* 26(4):447–452. doi:[10.1109/48.972077](https://doi.org/10.1109/48.972077)
- Weisstein EW (2002) *CRC concise encyclopedia of mathematics*, 2nd edn. Chapman and Hall/CRC, pp 1990–1991
- Young JH, Wan KC (2013) RRT-based path planning with kinematic constraints of AUV in underwater structured environment. In: *Proceedings of 10th International Conference on Ubiquitous Robots and Ambient Intelligence (URAI 2013)*. doi:[10.1109/urai.2013.6677328](https://doi.org/10.1109/urai.2013.6677328)
- Yu X, Gen M (2010) Simple evolutionary algorithms. In: *Introduction to evolutionary algorithms*, 1st edn. Springer-Verlag, London, pp 15–24. doi:[10.1007/978-1-84996-129-5](https://doi.org/10.1007/978-1-84996-129-5)
- Zhang Z, Zhao Z (2014) A multiple mobile robots path planning algorithm based on A-star and Dijkstra algorithm. *Int J Smart Home* 8(3):75–86